2009

Utilizing Repeated GPS Surveys from Field Operations for Development of Agricultural Field DEMs

Samsuzana Abd Aziz
Iowa State University

Brian L. Steward
Iowa State University, bsteward@iastate.edu

Lie Tang
Iowa State University, lietang@iastate.edu

Manoj Karkee
Iowa State University

Utilizing Repeated GPS Surveys from Field Operations for Development of Agricultural Field DEMs

Abstract
Topographic data collected using RTK-DGPS-equipped farm vehicles during field operations could addadditional benefits to the original capital investment in the equipment through the development of high-accuracy field DEMs. Repeated surveys of elevation data from field operations may improve DEM accuracy over time. However, minimizing the amount of data to be processed and stored is also an important goal for practical implementation. A method was developed to utilize repeated GPS surveys acquired during field operations for generating field-level DEMs. Elevation measurement error was corrected through a continuity analysis. Fuzzy logic (FL) and weighted averaging (WA) methods were used to combine new surveys with past elevation estimates without requiring storage and reprocessing of past survey data. After 20 surveys were included, the DEM of the study area generated with FL and WA methods had an average root mean squared error (RMSE) of 0.08 m, which was substantially lower than the RMSE of 0.16 m associated with the DEM developed by averaging all data points in each grid. With minimum control of errors in elevation measurements, the effect of these errors can be reduced with appropriate data processing, including continuity analysis, fuzzy logic, and weighted averaging. Two years of GPS surveys of elevation data from field operations could reduce elevation error by 50% in field DEMs.

Keywords
Digital elevation model, Fuzzy logic, GPS, Topography

Disciplines
Agriculture | Bioresource and Agricultural Engineering

Comments
This article is from *Transactions of the ASABE*, 52, no. 4 (2009): 1057–1067.

UTILIZING REPEATED GPS SURVEYS FROM FIELD OPERATIONS FOR DEVELOPMENT OF AGRICULTURAL FIELD DEMS

S. Abd Aziz, B. L. Steward, L. Tang, M. Karkee

ABSTRACT. *Topographic data collected using RTK-DGPS-equipped farm vehicles during field operations could add additional benefits to the original capital investment in the equipment through the development of high-accuracy field DEMs. Repeated surveys of elevation data from field operations may improve DEM accuracy over time. However, minimizing the amount of data to be processed and stored is also an important goal for practical implementation. A method was developed to utilize repeated GPS surveys acquired during field operations for generating field-level DEMs. Elevation measurement error was corrected through a continuity analysis. Fuzzy logic (FL) and weighted averaging (WA) methods were used to combine new surveys with past elevation estimates without requiring storage and reprocessing of past survey data. After 20 surveys were included, the DEM of the study area generated with FL and WA methods had an average root mean squared error (RMSE) of 0.08 m, which was substantially lower than the RMSE of 0.16 m associated with the DEM developed by averaging all data points in each grid. With minimum control of errors in elevation measurements, the effect of these errors can be reduced with appropriate data processing, including continuity analysis, fuzzy logic, and weighted averaging. Two years of GPS surveys of elevation data from field operations could reduce elevation error by 50% in field DEMs.*

Keywords. *Digital elevation model, Fuzzy logic, GPS, Topography.*

In agricultural practices, accurate representation of field topography is useful to implement precision agriculture management for more efficient production systems. Topographical information is important because it provides derived parameters such as slope, aspect, topographic index, and flow accumulation that are critical for agricultural conservation planning. For example, the movement of sediment, soil particles and agricultural chemicals (Maidment, 1996), and crop residue cover (Brown, 2008) are closely linked to soil topography and slope. In practice, topographic maps in the form of digital elevation models (DEMs) have been used to assess transport of constituents such as sediment and surface runoff from forested and agricultural watersheds (Ghidey et al., 2001; Ouyang et al., 2005; Sarangi et al., 2007), derive potential flow accumulation to assess soil moisture patterns and soil texture changes in a field (Schmidt and Persson, 2003), and estimate soil erosion for appropriate farm management and soil water conservation planning (de Jong et al., 1999; Oost et al., 2000; Lin and Lin, 2001; Ritsema et al., 2001). In spite of the importance of DEMs in agriculture, it is nevertheless a challenge to obtain elevation data cost-effectively with sufficient accuracy and resolution.

Submitted for review in June 2009 as manuscript number PM 7330; approved for publication by the Power & Machinery Division of ASABE in June 2009.

The authors are **Samsuzana Abd Aziz,** Senior Lecturer, Department of Biological and Agricultural Engineering, Faculty of Engineering, Universiti Putra Malaysia, Serdang, Selangor Darul Ehsan, Malaysia; **Brian L. Steward, ASABE Member Engineer,** Associate Professor, **Lie Tang, ASABE Member Engineer,** Assistant Professor, and **Manoj Karkee, ASABE Member Engineer,** Doctoral Candidate, Department of Agricultural and Biosystems Engineering, Ames, Iowa. **Corresponding author:** Brian L. Steward, Department of Agricultural and Biosystems Engineering, Iowa State University, 214D Davidson, Ames, IA 50011; phone: 515-294-1452; fax: 515-294-2255; e-mail: bsteward@iastate.edu.

A DEM is a digital representation of land topography representing elevations on the earth's surface. A DEM can be represented by one of three data structures: (1) gridded models, in which elevation is estimated for each point on a regular grid; (2) triangulated irregular networks (TIN), in which terrain elevation is represented in a network of non-overlapping irregular triangles; and (3) contour-based networks, in which landscape is divided into small, irregularly shaped polygons based on natural contour lines and their orthogonals (Wilson and Gallant, 2000). The square-grid (gridded) model is the most common form of DEM because of its simplicity and ease of computer implementation (Wise, 1998). This article is therefore focused on developing gridded DEMs and, for simplicity, the term DEM will be used to refer to them.

Traditionally, DEMs were developed using elevation data collected from conventional surveying techniques such as theodolite and level surveys. Currently, remote sensing techniques, such as traditional aerial photogrammetric surveys, airborne laser scanning (Ackermann, 1999), synthetic aperture radar (SAR; Evans and Apel, 1995), and light detection and ranging (LiDAR; Vaze and Teng, 2007) are often used. Remote sensing techniques require less labor, but using these data sources to represent the topography of a particular site is often too expensive and may require considerable technical and computer expertise for appropriate data handling and processing. Usually, DEMs can be purchased from a service provider such as the U.S. Geological Survey (USGS), which sells DEMs at varying levels of accuracy. USGS 7.5-minute DEMs, with grid spacing of 10 m or 30 m, are the most accurate, with root mean squared error (RMSE) of 7 m and 15 m, respectively, and have been produced by interpolating elevations from vectors or digital line graph hypsographic and hydrographic data.

The advent and widespread use of the Global Positioning System (GPS) in agriculture provides new and affordable op-

  ISSN 0001–2351

portunities for farmers to collect elevation data. Every time GPS-equipped vehicles are operated in the field, elevation data can be recorded. The ability to obtain elevation data using GPS-equipped farm vehicle offers great advantages, as surveys can be done during the course of other field operations and thus do not require additional time or labor for data collection. In 1992, real-time kinematic differential GPS (RTK-DGPS) became commercially available with measurement capabilities within 1 to 4 cm accuracy (Buick, 2006). RTK-DGPS is becoming more widely adopted, as many applications in precision agriculture require high accuracy and consistent positional data. Auto-guidance systems used in row crops, for example, require high-accuracy positional measurements because cultivation, strip-tillage, and harvesting must follow the planted rows precisely. In addition, the use of GPS receivers in agriculture is expected to shift toward RTK-DGPS as greater coverage of RTK networks comes available.

Several studies have investigated the feasibility of using vehicle-mounted RTK-DGPS receivers to acquire topography data during typical field operations to generate DEMs. Clark and Lee (1998) compared DEMs produced from stop-and-go measurements with DEMs developed from kinematic measurements collected using an RTK-DGPS receiver mounted on a moving vehicle. They showed that kinematic measurements produced DEMs with slightly higher error (3 to 8 cm), but the increase was minimal relative to the amount of additional effort required to collect stop-and-go (error of 2 to 3 cm) measurements. Westphalen et al. (2004) used RTK-DGPS receivers and an inertial measurement unit (IMU) mounted on an agricultural sprayer to measure vehicle attitude and elevation data to generate DEMs. With the combination of IMU and the kinematic GPS measurements, the RMSE of the DEMs ranged from 10 to 15 cm.

As a growing proportion of agricultural vehicles are equipped with GPS receivers, elevation data may be gathered continuously during common field operations. The accuracy of elevation data and any derived parameters can be improved using repeated surveys and averaging GPS point locations over several years (Renschler et al., 2002). Repeated GPS surveys of elevation data from field passes of agricultural vehicles could be advantageous in improving the accuracy of the DEM. However, with repeated surveys comes the challenge of handling increasingly larger amounts of data, particularly if all of the data are required for improving DEM accuracy. Moreover, vertical and horizontal position measurement errors might occur in each survey due to device inaccuracies and human error during data collection.

To address these issues, algorithms were developed to combine repeated GPS surveys for improving elevation estimates of agricultural fields. We proposed a process that would minimize user input and intervention and as well as expertise requirements for generating field-level DEMs as a by-product of GPS equipped field operations. The goal of this research was to develop a methodology of combining repeated GPS surveys from field operations for the development of agriculture field DEMs. The specific objectives of the research were: (1) to compare fuzzy logic, weighted averaging, and grid-wise averaging techniques for combining repeated GPS surveys; and (2) to observe the effect of combining multiple GPS surveys over several years on DEM accuracy.

Data Simulation and Collection

The methods proposed in this study were tested using elevation data from two sources:

Simulated RTK-DGPS elevation surveys: RTK-DGPS elevation surveys were simulated to provide datasets for methodology development. Elevation values were interpolated from a USGS DEM along predefined field operation paths to simulate the GPS surveying process. RTK-DGPS errors were modeled and added to these simulated measurements. Simulated survey data were used to focus on the effects of GPS errors inherent in GPS measurements. With these data, it was assumed that the USGS DEM was the best elevation representation for that area, and it was thus used as the true surface for validation.

Experimental RTK-DGPS field surveys: To test the algorithm on measured data, multiple GPS surveys were conducted on a test field by driving an agricultural vehicle with RTK-DGPS receivers mounted on it. Another set of GPS surveys was collected using an RTK-DGPS receiver mounted on a sled pulled by a utility vehicle. The measurements from this latter set of surveys were used as reference measurements for validation. They were collected closer to the ground to minimize the errors due to vehicle dynamics and geometry associated with the test measurements.

Simulated RTK-DGPS Elevation Surveys

A test field was modeled using a 7.5-minute USGS DEM of Winneshiek County, Iowa, with 10 m grid spacing. The USGS DEM was acquired from an online GIS data provider (GeoCommunity, 2007). Most of the area in Winneshiek County consists of farm land (380,034 acres; 86% of the total area). A 120 × 120 m area with elevation ranging from 1117 to 1124 m (around 8 m elevation difference) was selected (fig. 1) for the study because it contained some topographical relief but did not contain features such as streams, rivers, or lakes that would prevent contiguous farm operations. To simulate surveys occurring during field operations, vehicle travel paths were predefined based on four field operations (tillage, planting, spraying, and harvesting) typical of a corn-soybean rotation in Iowa (fig. 2). Elevation values were then interpolated at each sampling location on the defined paths using inverse distance weighting (IDW) interpolation. Data were sampled along straight north-south paths for planting, spraying, and harvesting operations and along diagonal northeast-southwest paths for tillage operations. The swath spacing was 6.1 m for planting, harvesting, and tillage operations and 27.4 m for spraying operations (table 1). The distance between data points along the path was 0.5 m, based on a 5 Hz measurement rate with 9.7 km h^{-1} vehicle speed. For each dataset, the sampling path started near the southwest corner of the field, where the first sample point of the path was generated at a random distance off of a fixed starting point (normally distributed with $\sigma = 0.5$ m). Thus, the location of the sampling path was in general different for each dataset. This variation was added because the field operations were assumed to be non-controlled traffic operations in which the exact positions of the track operations will vary each year. At each simulated sampling location, a five-dimensional vector was generated consisting of easting, northing, elevation, DGPS station ID number, and sampling time. A total of 20 simulated GPS measurement surveys (corresponding to five years of field operations) from the area

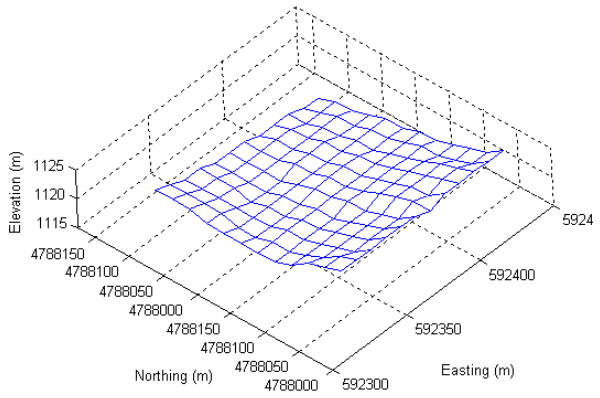

Figure 1. Digital elevation model for the study area from Winneshiek County, Iowa. The standard USGS Universal Transverse Mercator (UTM) format was used with UTM grid zone of 15N for the coordinate projection using North American Datum 1983 (NAD1983).

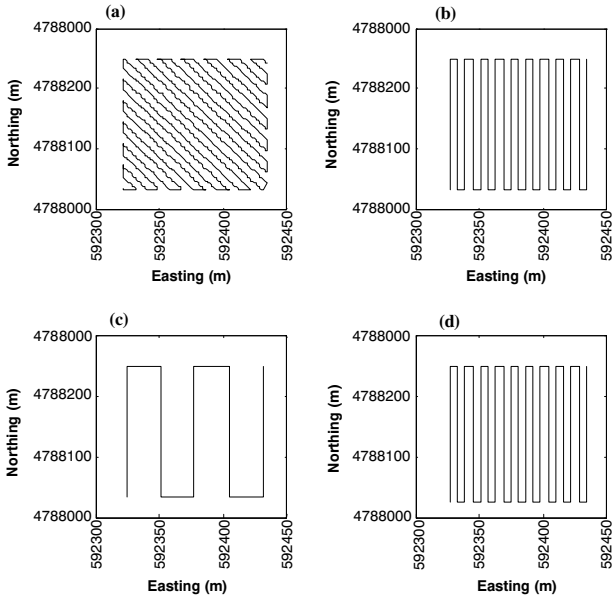

Figure 2. Diagonal (northeast-southwest) sampling path for (a) tillage and straight (north-south) sampling patterns for (b) planting, (c) spraying, and (d) harvesting operations in the study area.

Table 1. Machine and track specifications used in simulating the elevation data.

Machine	Track Width (m)	Track Direction
Chisel plow tillage	6.10	Diagonal (northeast-southwest)
Planter (8 row, 30 inch spacing)	6.10	Straight (north-south)
High-clearance sprayer	27.43	Straight (north-south)
Harvester (8 row, 30 inch spacing)	6.10	Straight (north-south)

were generated with simulated GPS noise added to the datasets. This process was replicated three times for analysis.

Vehicle-based RTK-DGPS system accuracy relies on GPS signal quality and continued availability of the differential correction signal. Loss or interruption of the DGPS correction signal will affect the GPS positioning measurement,

Table 2. Pseudorange error statistics for DGPS error modeling (James, 1994).

	Gauss-Markov Noise		Measurement Noise
	SD, σ (m)	Time, τ (s)	SD, σ (m)
RTK-DGPS position error	0.096	600	0.0038
Discontinuity error (dual-frequency P-code)	1.030	600	0.3160

which introduces errors in the range of centimeters (Scherzinger et al., 2007). Errors may also occur when satellites appear or leave the field of view during the GPS data collection. In our previous work, when the RTK-DGPS receiver lost the correction or satellite signal, the receiver mode automatically changed from fixed to float DGPS correction solution (lower accuracy), which introduced large discontinuities in the measurements along the vertical and horizontal planes. We modeled this noise using pseudorange error statistics for a dual-frequency P-code DGPS receiver. This noise together with the kinematic DGPS position errors are usually represented as stochastic errors that are correlated in time (Farrell and Barth, 1999). In this study, Gauss-Markov processes (James, 1994) were used to model the errors because their exponential time-correlation function holds the properties of the errors. The Gauss-Markov terms were modeled as:

$$\varepsilon_i = \varepsilon_{i-1} e^{-\Delta T/\tau} + w_i \quad (1)$$

where

ε_i = ith error
ε_{i-1} = $(i-1)$th error
w_i = RTK-DGPS measurement noise represented as random process drawn from a normal distribution
ΔT = sampling interval.

These processes can be described as an exponential autocorrelation function with variance σ^2 and time constant τ (table 2):

$$R(t) = \sigma^2 e^{-|t|/\tau} \quad (2)$$

Three independent random number generators were used to produce normally distributed random noise. The first random number generator provided the Gauss-Markov noise related to RTK-DGPS errors. The second random number generator produced the Gauss-Markov noise for the discontinuity errors. The discontinuity noise was turned on for six to ten times at 5 s intervals by generating random numbers indicating when the noise would occur in the samples (fig. 3). The third random number generator produced the GPS measurement noise (w_i) with standard deviation (SD) $\sigma = 0.316$ m when the discontinuity noise was turned on and $\sigma = 0.0038$ m when the discontinuity noise was turned off (James, 1994). These error models were added to the simulated elevation surveys. Errors were modeled independently along each *X*, *Y*, and *Z* measurement axis. The survey simulation algorithm was written in Matlab version 7.0 (The Mathworks, Inc., Natick, Mass.).

Experimental RTK-DGPS Field Surveys

Multiple GPS surveys were collected from a small portion of a grassy field in Ames, Iowa. The field of interest covered an area of 0.23 ha (36.56 m wide × 60.96 m long) and had a 0° to 8° slope, which was oriented to the southwest. The elevation ranged from 323 m to about 326 m. Elevation data

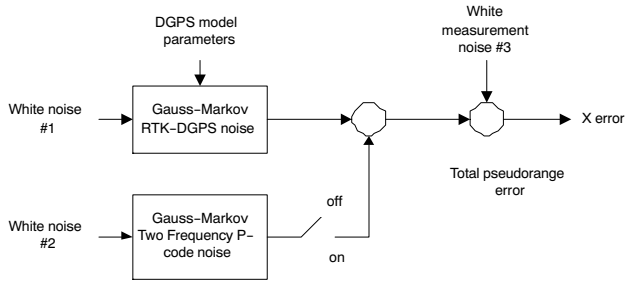

Figure 3. Algorithm for producing error in *X* axis (*Y* and *Z* axes are similar; James, 1994).

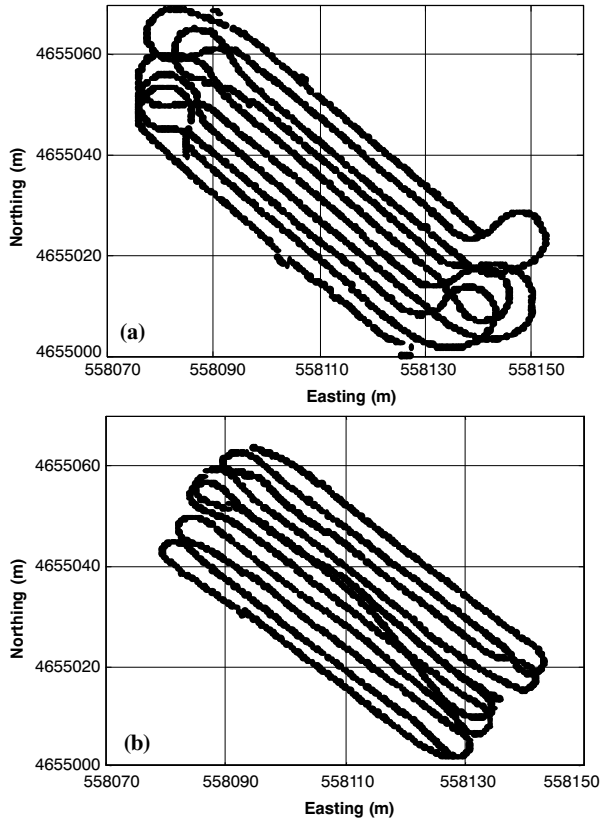

Figure 4. Data collection tracks in the study area using (a) an agricultural sprayer with 1 Hz RTK-DGPS receivers and (b) a custom-developed sled pulled by a John Deere utility vehicle with a 5 Hz RTK-DGPS receiver (used as the validation set).

were collected using a self-propelled high-clearance agricultural sprayer (*ASABE Standards*, 2005) equipped with RTK-DGPS receivers (StarFire RTK, Deere & Co., Moline, Ill.) operating at 1 Hz with a vertical static RMSE of less than 1.5 cm. The GPS receivers were mounted at a height of 3.8 m above the field surface. The vehicle was driven across the field at a speed of 3.2 to 14.5 km h^{-1} along passes that were 3.05 m apart (fig. 4). Correction signals were sent from the local base station via a radio link (Pacific Crest Corp., Santa Clara, Cal.) The base station was located at 61 m northwest of the test field. A total of 16 datasets of field surveys were collected.

Another set of independent surveys across the entire field was collected for validation. These reference measurements were acquired using an RTK-DGPS receiver operating at 5 Hz on a custom-built sled. A John Deere utility vehicle (Gator, Deere & Co., Moline, Ill.) was used to pull the sled across the field at 6.4 to 9.7 km h^{-1}. These measurements were collected closer to the ground to eliminate the errors caused by the vehicle dynamics contained in the test data. In general, as a vehicle travels over a field's topography, weight transfer leads to changes in vehicle pitch or roll angles relative to the slope based on the suspension stiffness. As such, the resulting elevation measurements have an additional error source associated with the vehicle suspension system and geometry. Since the reference measurements were collected using a GPS receiver mounted on a sled, these errors were minimized.

Since the raw data were in the format of a geographic coordinate system consisting of longitude, latitude, and altitude, the data were converted into a projected coordinate system. Projection was required for spatial data analysis using units of length in the horizontal plane. The standard USGS Universal Transverse Mercator (UTM) format was used (UTM grid zone 15N; NAD1983).

METHODS

A program was written in Matlab version 7.0 (The Mathworks, Inc., Natick, Mass.) to implement the methodology for generating field DEMs using repeated GPS surveys. The procedure consisted of the following steps (fig. 5):

Discontinuity detection: When an RTK-DGPS receiver lost the correction signal, the receiver mode changed from fixed to float mode solution (lower accuracy) and introduced discontinuous measurements in the dataset. A GPS discontinuity error correction algorithm was developed to correct these discontinuities.

DEM generation: Next, kriging interpolation was used to interpolate GPS measurements into gridded DEMs. A DEM was developed from each GPS elevation survey.

DEM combination and reduction: This study was based on the hypothesis that field DEM accuracy can be improved by combining the DEM estimates over several surveys. However, simply averaging the DEM estimates from different surveys may not be the best approach because one measurement survey may contain more error than another. Hence, two data combination algorithms were developed: one using a fuzzy logic (FL) approach and the other using a weighted average (WA) approach to combine data. Both methods only kept the current grid elevation estimates and their standard deviation and did not require data from previous surveys to be stored and reprocessed every time new GPS survey data became available. This feature is essential for practical implementation. DEMs were also developed through averaging the elevation at each grid (grid-wise averaging) to compare with the FL and WA results. Finally, a control method was used to develop a control DEM through grid-wise averaging without discontinuity analysis. Detailed explanations of each step are provided in the following sections.

DISCONTINUITY DETECTION

An algorithm was developed to detect measurement discontinuity noise for data correction. In previous studies, the RTK-DGPS receiver introduced large discontinuities in the elevation measurements when changes from a fixed

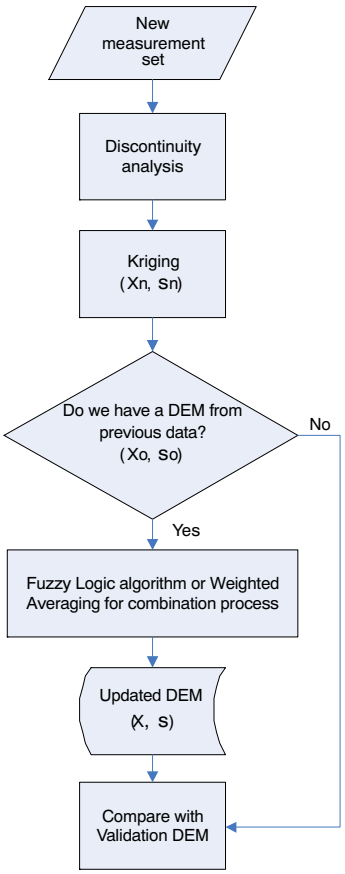

Figure 5. Overview of DEM development process using repeated surveys of elevation measurements. Each new measurement survey is combined with the existing DEM to improve the elevation estimate while reducing the amount of data to be stored.

solution to a float solution occurred. The DGPS reference station ID number also changed, and thus discontinuities were identified by finding the changes in the station ID. The points with a float solution ID were characterized as the discontinuity noise. Then the discontinuities in the *X* and *Y* axes were corrected by adjusting the coordinates to follow the coordinates direction of the vehicle path. The discontinuities in the elevation were corrected by re-estimating the value using the mean of eight nearest continuous neighboring points (points with fixed solution ID). Eight neighboring points were used because the horizontal distance between them and the corrected point was generally less than 3 m. Choosing more than eight neighboring points may involve points that are too far away from the corrected point and did not provide substantial improvement in the correction. To ensure that the discontinuities were minimized, the differences between adjacent elevation points along the path were computed. The discontinuities were minimized if the differences between the adjacent points along the path were within two standard deviations of the mean elevation differences. The result of this process can be seen through inspection of the elevation plot (fig. 6).

KRIGING INTERPOLATION

After discontinuities were removed, cleaned elevation measurements were interpolated to generate a DEM. The DEM grid locations were pre-defined so that each DEM developed using measurements from a new survey would use the same grid locations. Elevation measurements were interpolated into the gridded DEM using ordinary kriging, which was chosen because it is commonly used and is shown, based on geostatistical theory, to be an unbiased estimator that minimizes error variance (Isaaks and Srivastava, 1989). In addition, visual inspection of the data indicated no large trends, and ordinary kriging is known to be quite robust (Trangmar et al., 1985). A Matlab kriging toolbox (Sidler, 2003) was used with the von Kármán covariance model (von Kármán, 1948) instead of a common semivariogram model to describe the spatial structure of the data. For our implementation, in which sampled data were located preferentially and had a high possibility of outliers due to uncertainty in GPS measurements, the covariance model was appropriate. In a deterministic framework, where available sample information is interpolated within the same domain, direct estimation of the covariance model is better than the traditional semivariogram approach because the covariance estimator is less sensitive to extreme values, skewed distributions, and clustered sampling than the traditional semivariogram estimator (Isaaks and Srivastava, 1998).

For the simulated GPS surveys, data were fit with an exponential covariance model with a 20 m range. Data points were interpolated to 10 m grids using a minimum of 16 data points. For experimental field surveys, data points were interpolated to 1 m grids with similar kriging parameters. The range distance, grid size, and number of data points represented a trade off between interpolation support and computation time. Anisotropy was taken in account as the search neighborhood was defined as an ellipse centered on the location being estimated and rotated with the major axis in the vehicle path direction. The kriging elevation estimate and kriging variance for each grid were stored.

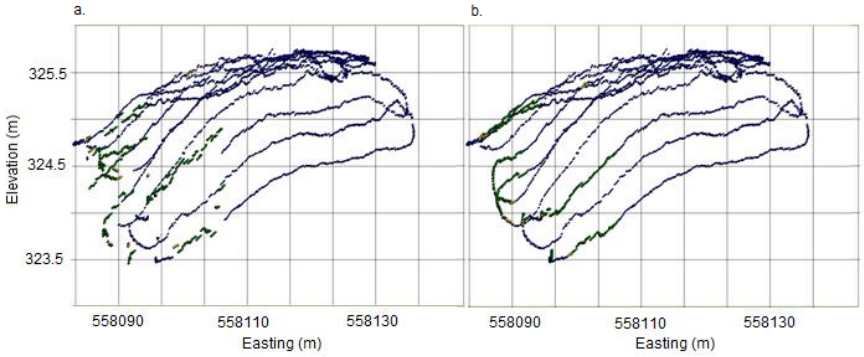

Figure 6. Elevation measurements (a) before and (b) after discontinuity analysis on a measurement survey collected at the study area.

Data Combination and Reduction

After the kriging interpolation, the DEM estimates from different GPS surveys were combined using FL and WA methods. Both methods were developed for improving statistical estimates as new information comes available while not requiring storage of all prior measurements.

Fuzzy Logic Method

The process of combining the elevation estimates from two DEMs used a fuzzy logic algorithm to take into account the uncertainty at each grid represented by the kriging variance at each grid. Specifically, the algorithm adjusted the elevation estimate of a grid with higher kriging variance to be at least within two standard deviations of the grid estimate with a lower kriging variance from the other DEM. Kriging variance is the minimized estimation error variance under the condition of unbiasedness. The error variance is estimated based on the underlying semivariogram model. A smaller kriging variance indicates that the kriging estimate is more strongly supported by elevation measurements and thus more accurately represents the true elevation. Hence, the purpose of adjusting the higher variance grid estimate to within two standard deviation of that with a lower variance is to improve the accuracy of the DEM in the sense that the elevation estimate with lower kriging variance is better supported by measurements than that with a higher kriging variance.

The lower kriging variance grid estimate was used as the base estimate, x_1. Then the grid estimate from the other DEM, x_2, was categorized into low, average, and high uncertainty fuzzy classes using a set of fuzzy membership functions developed in a similar approach (Zhang and Han, 2002). The fuzzy membership functions represented the difference between two grid kriging estimates (fig. 7):

$$\mu_L(x_2)=\begin{cases} 1, & x_2 \le x_1 - 2\sigma_{x_1} \\ 1-2\left(\dfrac{(x_1-2\sigma_{x_1})-x_2}{2\sigma_{x_1}}\right), & x_1-2\sigma_{x_1} < x_2 \le x_1-\sigma_{x_1} \\ 2\left(\dfrac{x_1-x_2}{2\sigma_{x_1}}\right)^2, & x_1-\sigma_{x_1} < x_2 \le x_1 \\ 0, & x_2 > x_1 \end{cases} \quad (3)$$

$$\mu_A(x_2)=\begin{cases} 0, & x_2 \le x_1 - 2\sigma_{x_1} \\ 2\left(\dfrac{(x_1-2\sigma_{x_1})-x_2}{2\sigma_{x_1}}\right)^2, & x_1-2\sigma_{x_1} < x_2 \le x_1-\sigma_{x_1} \\ 1-2\left(\dfrac{x_1-x_2}{2\sigma_{x_1}}\right)^2, & x_1-\sigma_{x_1} < x_2 \le x_1+\sigma_{x_1} \\ 2\left(\dfrac{(x_1+2\sigma_{x_1})-x_2}{2\sigma_{x_1}}\right)^2, & x_1+\sigma_{x_1} < x_2 \le x_1+2\sigma_{x_1} \\ 0, & x_2 > x_1+2\sigma_{x_1} \end{cases} \quad (4)$$

$$\mu_H(x_2)=\begin{cases} 0, & x_2 \le x_1 \\ 2\left(\dfrac{x_1-x_2}{2\sigma_{x_1}}\right)^2, & x_1 < x_2 \le x_1+\sigma_{x_1} \\ 1-2\left(\dfrac{(x_1+2\sigma_{x_1})-x_2}{2\sigma_{x_1}}\right)^2, & x_1+\sigma_{x_1} < x_2 \le x_1+2\sigma_{x_1} \\ 1, & x_2 > x_1+2\sigma_{x_1} \end{cases} \quad (5)$$

where μ_L, μ_A, and μ_H are the degrees of membership (DOM) for the low, average, and high fuzzy classes, respectively, and σ_{x1} and σ_{x2} are the standard deviations associated with the grid kriging variance from the two DEMs. The average class indicates that the estimate is within two standard deviations of the kriging estimate of the lower kriging variance grid and data correction may not be necessary. Elevation estimates with high degrees of membership in the high or low classes, however, can be corrected by shifting them to be similar to the kriging estimate of the grid with lower variance.

The DOMs were used as the inputs to a fuzzy model to produce a crisp output to be used as a weight for data correction. The membership functions of the fuzzy output classes consisted of trapezoid and triangle shapes where the output variable u was between –1 and 1 (fig. 8). The inference of input to the output was based on the following rules:

- If elevation estimate x_2 is low, then output variable u is large negative shift.

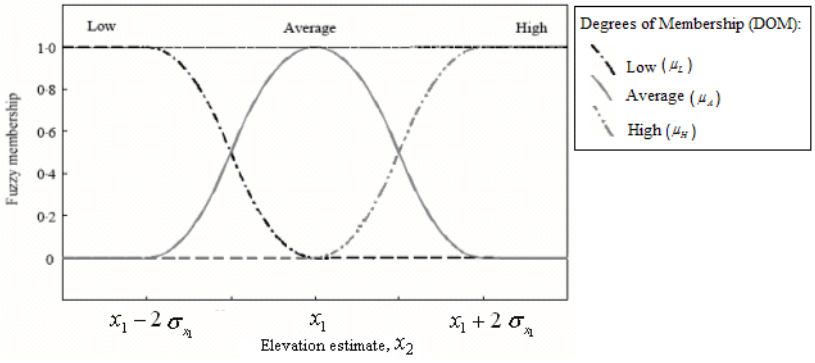

Figure 7. Graphical representation of fuzzy membership functions for low, average, and high elevation for estimate x_2 in relation to estimate x_1 in a grid, with standard deviation σ_{x1}.

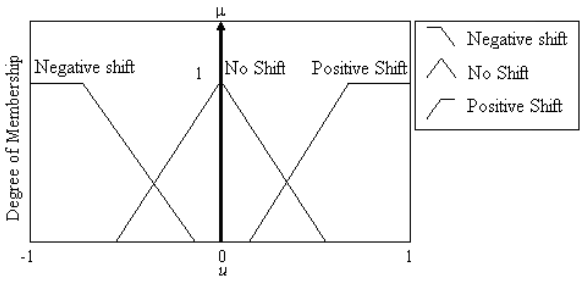

Figure 8. Fuzzy output model for determining the weight for data correction based on the degrees of membership μ(*u*) and output variable *u*.

- If elevation estimate x_2 is average, then output variable u is small shift.
- If elevation estimate x_2 is high, then output variable u is large positive shift.

The crisp output from this fuzzy model was determined using the centroid defuzzification technique defined as:

$$u^* = \frac{\sum_{i=L,A,H} \int_{-1}^{1} \mu_i(u) \cdot u du}{\sum_{i=L,A,H} \int_{-1}^{1} \mu_i(u) du} \quad (6)$$

where $\mu_i(u)$ is the DOM of the output membership function. The fuzzy output was then used as a weight in the correction function defined as:

$$x_2' = x_2 - u^* \cdot D_{x_2 - x_1} \quad (7)$$

where

x'_2 = corrected estimate
x_2 = kriging estimate of a grid
u^* = weight obtained from fuzzy logic algorithm
$D_{x\,2\,-\,x\,1}$ = absolute differences between x_2 and x_1.

After data correction using fuzzy logic, the estimates x'_2 and x_1 were averaged and stored. Since the accuracy of x_2 estimates were improved using the fuzzy algorithm relative to the x_1 estimate, the variance of the combined estimates was represented by σ_{x1}, the kriging variance associated with x_1. This variance was passed along to be used for analysis when the next DEM was available. This process was repeated for all the grids of the study area. The process kept the current estimate of the elevation in each grid and its associated variance, and thus no additional prior data were required for future DEM recombination with new survey measurements.

Weighted Averaging Method

In the WA method, DEMs were combined grid-wise using a weighted average function defined as:

$$x_\mu = \left(\frac{\sigma_{x_2}^2}{\sigma_{x_1}^2 + \sigma_{x_2}^2} \right) x_1 + \left(\frac{\sigma_{x_1}^2}{\sigma_{x_1}^2 + \sigma_{x_2}^2} \right) x_2 \quad (8)$$

where x_μ is the new estimate (combination) of the elevation of the grid, and x_1 and x_2 are the estimates from the two DEMs.

The variance of the combined estimate, σ_μ^2, was then defined as:

$$\sigma_\mu^2 = \left(\frac{\sigma_{x_1}^2 \sigma_{x_2}^2}{\sigma_{x_1}^2 + \sigma_{x_2}^2} \right) \quad (9)$$

From equation 9, the updated variance is less than the smallest input variance since:

$$\frac{1}{\sigma_\mu^{\,2}} = \left(\frac{1}{\sigma_{x_1}^2} \right) + \left(\frac{1}{\sigma_{x_2}^2} \right) \quad (10)$$

The averaging function weighted the estimate based on the kriging variance, so if the kriging variance of a particular grid from DEM 1, x_1, is greater than that from DEM 2, x_2, then x_2 contributes more than x_1 to x_μ. From equation 10, the standard deviation σ_μ is less than either σ_{x1} or σ_{x2}, which implies that the uncertainty in the estimate decreases by combining the two pieces of information. This process was repeated for all the grids of the study area, and the same procedure was used when new surveys were acquired. The process only kept the current estimate of the elevation in each grid and its associated variance. It did not require all previous data to be stored and reprocessed every time new surveys were acquired.

Accuracy of DEM Elevations

Root mean squared error (RMSE), a typical measure of DEM error (Wise, 1998; Bishop and McBratney, 2002; Wilson et al., 2005; Westphalen et al., 2004), was used to measure the performance of the various methods in producing accurate DEMs. For the simulated GPS surveys, the original USGS DEM data were used as the validation values for each DEM grid, and error was calculated by subtracting the elevation estimates from the USGS DEM values. For the DEMs developed using multiple GPS surveys, error was calculated by subtracting the DEM estimates from the nearest reference measurement value.

Results and Discussion

DEMs Developed from Simulated RTK-DGPS Elevation Surveys

The contour map of the DEMs produced using the control method exhibited some artifacts that were most obvious in the northern half of the field (fig. 9a). The contour lines at the north of the field were not as smooth if compared to the contour lines in the map developed using reference data (fig. 10a). These artifacts were mainly due to the discontinuity noise in the measurements, which was not removed in the control process. The RMSE of the DEM developed using the control method was substantially high, with an average maximum value of 1.38 m, when a single simulated elevation survey was used to generate the DEM. The average RMSE from three replications decreased to 0.40 m after 20 simulated surveys were used (fig. 9b). With proper data-processing techniques, errors in the field measurements could be reduced to improve the DEMs accuracy.

The contour map generated with data from the original USGS DEM of the test field (fig. 10a) was compared with contour maps of the DEMs produced from the simulated surveys (fig. 10b, 10c, and 10d). The contour map of the grid-wise averaging DEM (fig. 10b) exhibited similar contour lines with a few artifacts or anomalies that seemed erroneous. However, with the FL and WA DEMs, most of the artifacts were removed (fig. 10d and 10c). These topographic maps had contour lines similar to the original USGS DEM contour

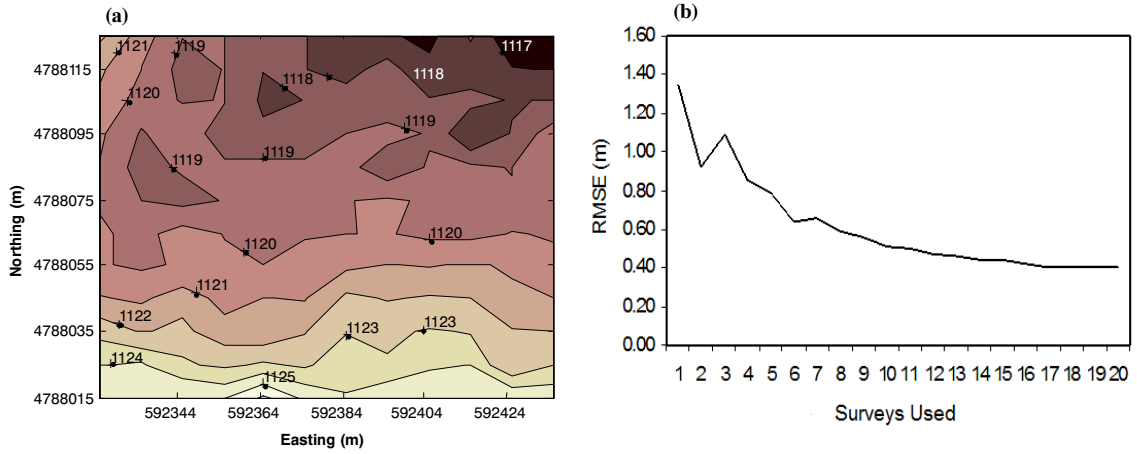

Figure 9. (a) Contour map of 10 m DEM of the test area from Winneshiek County produced by regularly averaging all data points in each grid without discontinuity error detection (control method) and (b) RMSE of the DEM as multiple GPS surveys were combined as they became available using the control process.

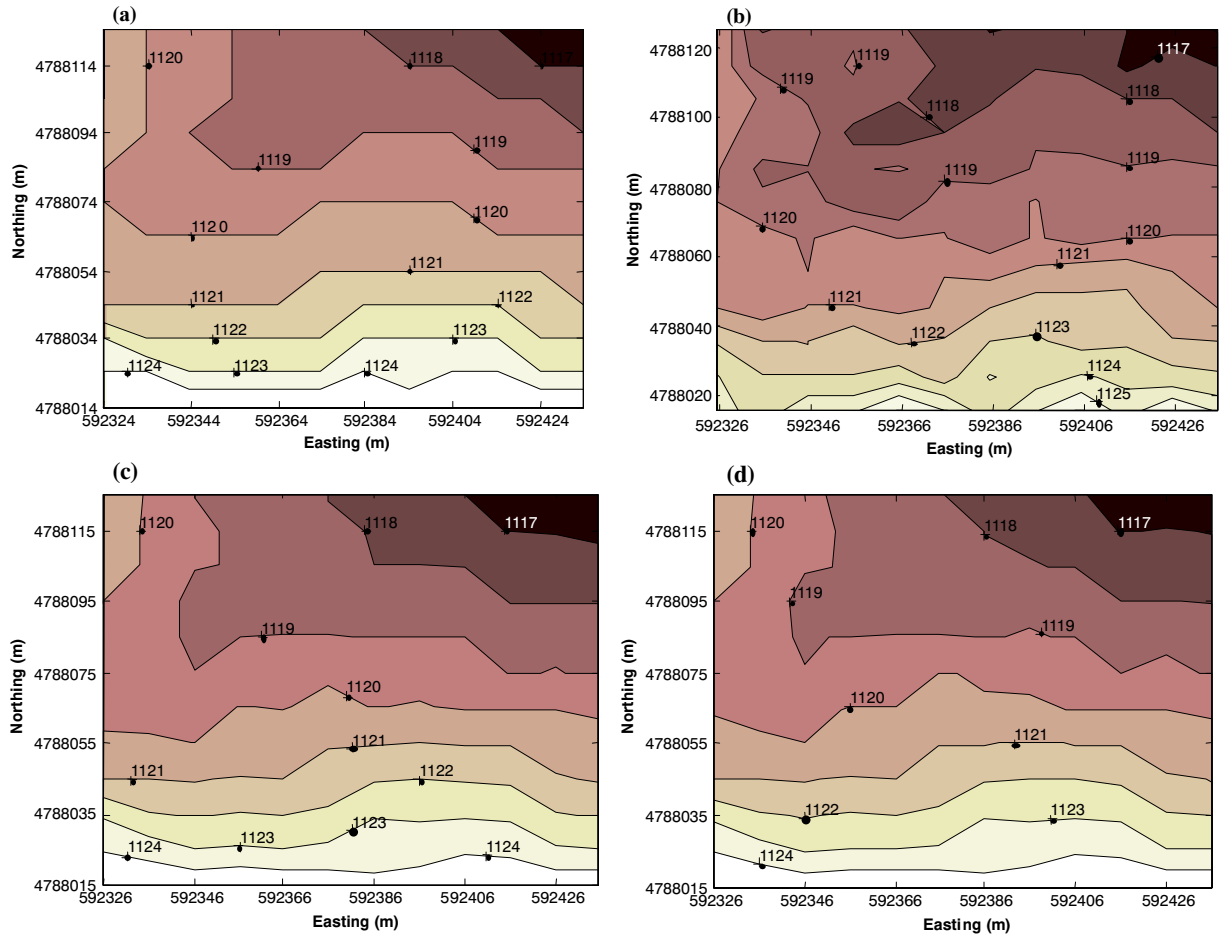

Figure 10. (a) Reference contour map compared to contour maps from DEMs produced by (b) grid-wise averaging method, (c) WA method, and (d) FL method.

map. It is obvious that data processing is needed to generate acceptable topographic maps from these simulated surveys.

The mean RMSE obtained from the DEM accuracy analysis for over three simulated measurement surveys decreased as the number of elevation surveys increased (fig. 11). DEMs developed using the grid-wise averaging method with discontinuity error detection had higher RMSE compared to DEMs developed using the FL and WA methods. Overall, from this plot, the RMSE for all methods decreased as the number of simulated elevation surveys increased. For the grid-wise averaging method, the average RMSE from three replications decreased from 0.34 m to 0.14 m after 20 surveys were used. For FL and WA methods, the average RMSE decreased from 0.28 m to 0.07 m and

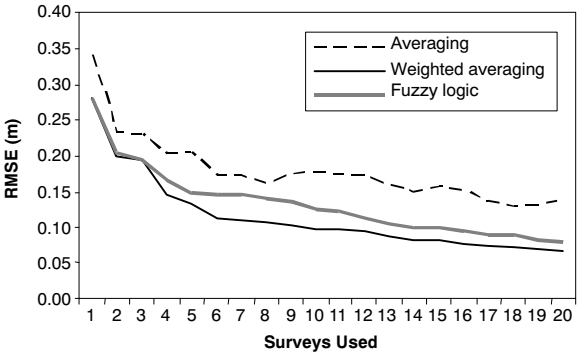

Figure 11. RMSE of DEMs as multiple simulated RTK-DGPS elevation surveys were combined using the methods developed in this study. RMSE were averaged from three independent replications.

0.08 m, respectively, as the number of elevation surveys used increased. For the first three surveys, the differences in RMSE between the FL and WA methods were very small. However, the RMSE from the WA method dropped lower than the FL method as more simulated elevation surveys were added. This lower error was due to how the variance was handled in each method. As more surveys were added, the WA method reduced the estimation variance through equation 9, while the FL method retained the minimum variance.

DEMs Developed from Experimental RTK-GPS Field Surveys

Similar analysis was done with the GPS surveys collected from the study area. Due to the discontinuity noise in the measurements, which was not removed in the control process, the contour map of the DEMs produced using the control method exhibited artifacts in the direction of the sampling pattern. (fig. 12a). The RMSE of the DEM developed using the control method was substantially high, with an average maximum value of 0.83 m. The RMSE varied substantially with a lower number of elevation surveys and became more stable at approximately 0.6 m as the number of surveys increased to five and above (fig. 12b).

The maps of DEMs developed using the grid-wise averaging, FL, and WA methods are displayed in figure 13. The algorithm robustly handled the error inherent in the GPS measurements, and the three methods had similar performance (fig. 14) as that observed with the simulated surveys. The DEMs developed using the grid-wise averaging method had substantially higher RMSE compare to the DEMs developed with the FL and WA methods. The RMSE for the grid-wise averaging method decreased from 0.21 m to 0.13 m after 20 surveys were used. The RMSE of DEMs developed using the FL and WA methods decreased from 0.20 m to 0.08 m as the number of surveys used increased (fig. 14). The differences in RMSE between these two methods were very small. However, the RMSE of the FL method DEM varied more than that of the WA method as new surveys were used.

Possible causes of other errors were the field conditions and vehicle dynamics. As the vehicle traveled over the field surface, it interacted with the micro-topography, the small-scale variance in the field surface. There were also variations in weight distribution of the vehicle from test to test, as data collections were conducted on the same vehicle path repeatedly and the soil surface was deformed as more passes were made. The temperature variation during data collection might also have caused changes in the air suspension system stiffness.

The effects of these errors were reduced when the DEMs were developed using the FL and WA methods. For the FL and WA methods, kriging produced an estimate by optimally weighting surrounding measurements. The grid-wise averaging method, however, is sensitive to outliers because it produced estimates by giving each measurement in a grid the same weight. Beyond initial estimation, the FL and WA methods were robust to outliers because in the data combination process, the kriging variance was passed along as a measure of confidence in the estimates based on prior sampling configurations. A smaller kriging variance indicated that the elevation estimate was more strongly supported by elevation measurements and thus should be more representative of the true elevation. When the estimates from different DEMs were combined, the FL method adjusted the estimate with less measurement support relative to that with more support before combining. The WA method weighted the estimates based on the confidence in the estimates during combination. Hence, these two methods

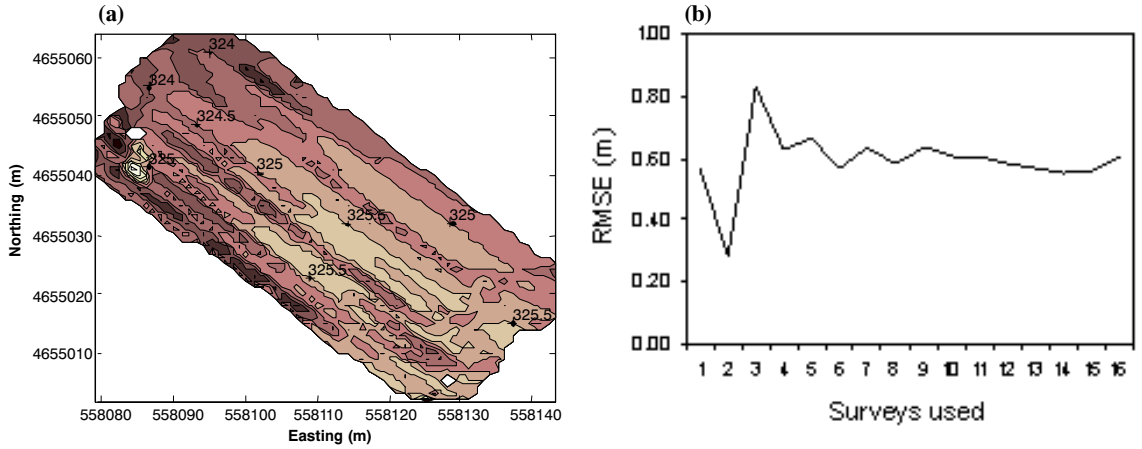

Figure 12. (a) Contour map of 1 m DEM of the study field by averaging all data points in each grid without discontinuity error detection (control process) and (b) RMSE of the DEM as multiple RTK-DGPS surveys were combined as they became available using the control process.

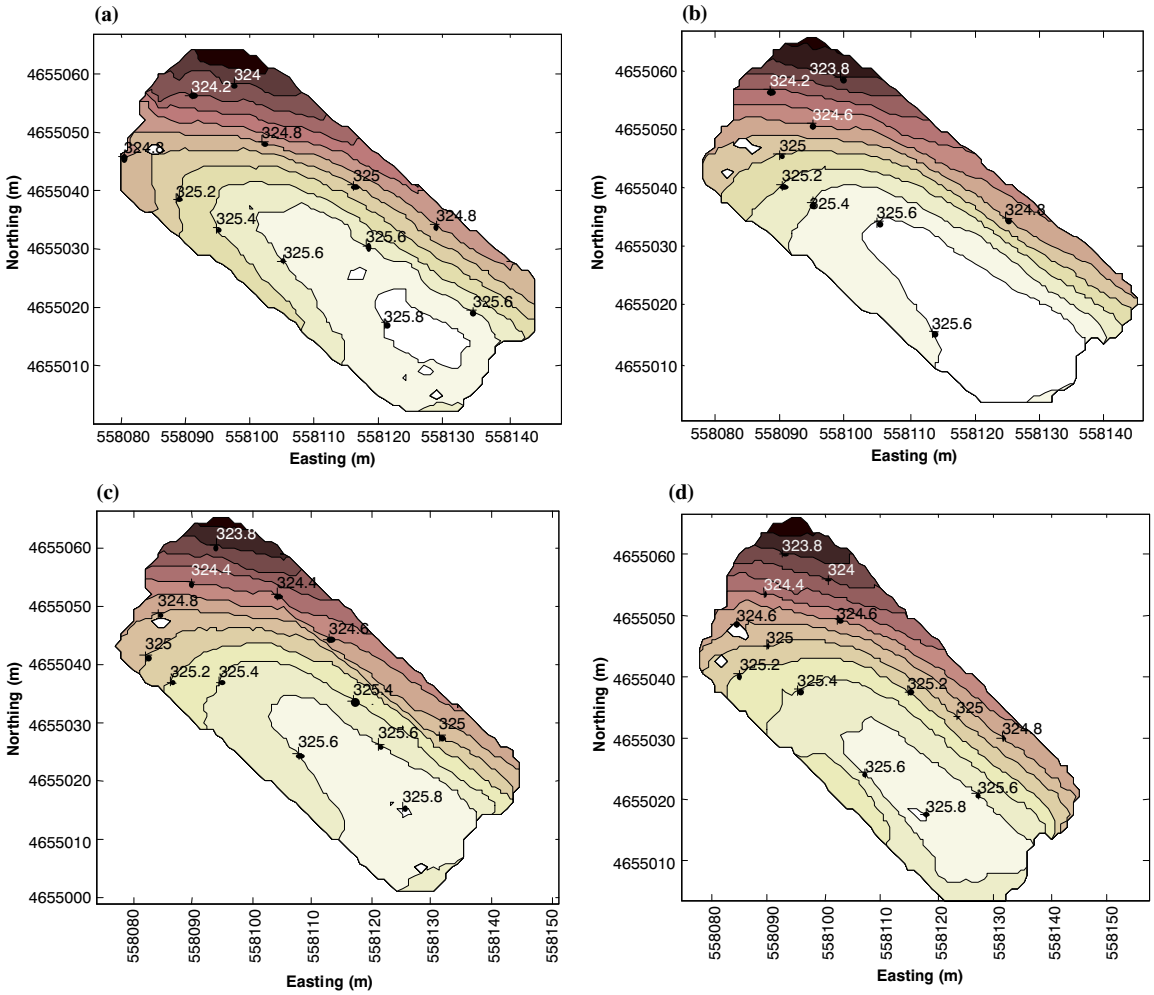

Figure 13. (a) Reference contour map compared to contour maps from DEMs produced by (b) grid-wise averaging method, (c) WA method, and (d) FL method using 16 surveys.

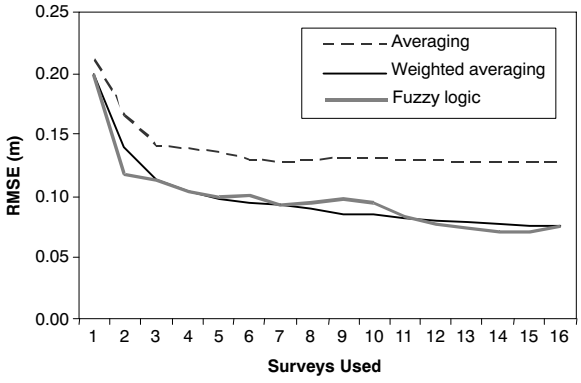

Figure 14. RMSE of DEMs as repeated RTK-DGPS surveys were combined using the methods developed in this study.

were more robust to measurement errors and resulted in improved performance over the grid-wise averaging method. This study demonstrates the importance of passing along a measure of estimate confidence in the process as measurements from new surveys are added.

CONCLUSION

GPS data surveys for the development of the field DEMs were simulated using publicly available USGS DEM and acquired using GPS-equipped farm vehicles. Repeated GPS surveys of elevation data improved the DEM accuracy over time. This article presented two methods for the development of field DEMs as a by-product of GPS-aided farm operations. These methods provided means to reduce the amount of raw elevation data passed on between measurements and combine them for improved elevation estimate. From this work, the following conclusions can be drawn:

- The DEMs from the experimental RTK-DGPS field surveys developed using the FL and WA methods had an average RMSE of 0.08 m after using 20 surveys, which was substantially lower than the RMSE of 0.60 m associated with the DEM developed by averaging all data points in each grid without discontinuity error detection. Overall, two years of GPS surveys of elevation data from field operations could improve the accuracy of the field DEM by 50% relative to the first DEM.
- With minimum control of errors in elevation measurement surveys, the effect of these GPS errors can be reduced with appropriate data processing to

reduce the effect of discontinuities and combine multiple survey data using methods that take into account the confidence in estimates based on their measurement support.
- With a large number of measurement surveys, the fuzzy logic and weighted averaging methods had about the same performance; however, DEM error associated with the weighted averaging method decreased more consistently as more measurement surveys were used.

ACKNOWLEDGEMENTS

This research of the Iowa Agriculture and Home Economics Experiment Station, Ames, Iowa (Project No. 3612) was supported by Hatch Act and State of Iowa funds and Malaysian Academic Staff Training (SLAB) scholarship from Malaysian Ministry of Higher Education.

REFERENCES

Ackermann, F. 1999. Airborne laser scanning: Present status and future expectations. *ISPRS J. Photogram. and Remote Sensing* 54(2-3): 64-67.

ASABE Standards. 2005. S390.4: Definition and classifications of agricultural field equipment. St. Joseph, Mich.: ASABE.

Bishop, T. F. A., and A. B. McBratney. 2002. Creating field-extent digital elevation models for precision agriculture. *Precision Agric.* 3(1): 37-46.

Brown, C. 2008. Plan a switch to less tillage. In *Wallaces Farmer* (Jan.), 19. Available at: www.wallacesfarmercom. Accessed 10 September 2008.

Buick, R. 2006. RTK base station networks driving adoption of GPS ±1 inch automated steering among crop growers. RTK network white paper. Westminster, Colo.: Trimble Agricultural Division. Available at: www.trimble.com. Accessed 31 March 2007.

Clark, R. L., and R. Lee. 1998. Development of topographic maps for precision farming with kinematic GPS. *Trans. ASAE* 41(4): 909-916.

de Jong, S. M., M. L. Paracchini, F. Bertolo, S. Folving, J. Megier, and A. P. J. de Roo. 1999. Regional assessment of soil erosion using the distributed model SEMMED and remotely sensed data. *Catena* 37(3-4): 291-308.

Evans, D. L., and J. Apel. 1995. Spaceborne synthetic aperture radar: Current status and future directions. A report to the Committee on Earth Sciences, Space Studies Board, National Research Council. NASA Technical Memorandum 4679. Pasadena, Cal.: NASA Jet Propulsion Laboratory. Available at: http://southport.jpl.nasa.gov/nrc/nrcT_of_C.html. Accessed 14 July 2003.

Farrell, J., and M. Barth, 1999. *The Global Positioning System and Inertial Navigation.* New York, N.Y.: McGraw-Hill.

GeoCommunity. 2007. USGS DEM Resources: 1995-2007. GIS Data Depot. Niceville, Fla.: MindSites Group. Available at: http://data.geocomm.com/. Accessed 23 April 2006.

Ghidey, E., E. E. Alberts, and L. A. Kramer. 2001. Comparison of measured and WEPP-predicted runoff and sediment loss from deep Loess soil watershed. In *Proc. Intl. Conf. on Soil Erosion Research*, 131-134. J. C. Ascough II and D. C. Flanagan, eds. St. Joseph, Mich.: ASAE.

Isaaks, E. H., and R. M. Srivastava. 1989. *An Introduction to Applied Geostatistics.* New York, N.Y.: Oxford University Press.

James, R. 1994. GPS and Differential GPS: An error model for sensor simulation. In *Proc. Position Location and Navigation Symposium*, 260-266. Piscataway, N.J.: IEEE.

Lin, C-Y., and W-T. Lin. 2001. An automated delineation of slope length for watershed upland erosion and sediment yield estimation. In *Proc. Intl. Conf. on Soil Erosion Research*, 423-426. J. C. Ascough II and D. C. Flanagan, eds. St. Joseph, Mich.: ASAE.

Maidment, D. R. 1996. GIS and hydrologic modeling: An assessment of progress. In *Proc. Intl. Conf. on Intergrating GIS and Environ. Modeling.* Available at: www.ce.utexas.edu/prof/maidment/gishydro/meetings/santafe/santafe.htm. Accessed 10 September 2008.

Oost, K. V., G. Govers, and P. Desmet. 2000. Evaluating the effects of changes in landscape structure on soil erosion by water and tillage. *Landscape Ecology* 15(6): 577-589.

Ouyang, D., J. Bartholic, and J. Selegan. 2005. Assessing sediment loading from agricultural croplands in the Great Lakes basin. *J. American Sci.* 1(2): 14-21.

Renschler, C. S., D. C. Flanagan, B. A. Engel, L. A. Kramer, and K. A. Sudduth. 2002. Site-specific decision-making based on RTK-GPS survey and six alternative elevation data sources: Watershed topography and delineation. *Trans. ASAE* 45(6): 1883-1895.

Ritsema, C. J., K. O. Trouwborst, V. Jetten, S. Ledin, L. Rui, L. Baoyuan, and F. Boije. 2001. An interdisciplinary approach for soil and water conservation planning to improve the sustainability of land-use on the Loess Plateau in China. In *Proc. Intl. Conf. on Soil Erosion Research*, 431-434. J. C. Ascough II and D. C. Flanagan, eds. St. Joseph, Mich.: ASAE.

Sarangi, A., C. A. Cox, and C. A. Madramootoo. 2007. Evaluation of the AnnAGNPS model for prediction of runoff and sediment yields in St Lucia watersheds. *Biosystems Eng.* 97(2): 241-256.

Scherzinger, B., J. Hutton, and M. Mostafa. 2007. Chapter 10: Enabling technologies. In *Digital Elevation Model Technologies and Applications: The DEM Users Manual*, 354-355. 2nd ed. D. F. Maune, ed. Bethesda, Md.: ASPRS.

Schmidt, F., and A. Persson. 2003. Comparison of DEM data capture and topographic wetness indices. *Precision Agric.* 4(2): 179-192.

Sidler, R. 2003. Kriging and conditional geostatistical simulation based on scaled-invariant covariance models. Diploma thesis. Zurich, Switzerland: Swiss Federal Institute of Technology, Institute of Geophysics, Department of Earth Science.

Trangmar, B. B., R. S. Yost, and G. Uehara. 1985. Application of geostatistics to spatial studies of soil properties. *Advances in Agron*. 38: 45-94.

Vaze, J., and J. Teng. 2007. High-resolution LiDAR DEM: How good is it? In *Proc. MODSIM 2007: Intl. Congress on Modelling and Simulation*, 692-698. L. Oxley and D. Kulasiri, eds. Modelling and Simulation Society of Australia and New Zealand. Available at: www.mssanz.org.au/MODSIM07/papers/12_s27/HighResolution_s27_Vaze_.pdf.

von Kármán, T. V. 1948. Progress in the statistical theory of turbulence. *Proc. Natl. Acad. Sci.* 34(11): 530-539.

Westphalen, M. L., B. L. Steward, and S. Han. 2004. Topographic mapping through measurement of vehicle attitude and elevation. *Trans. ASAE* 47(5): 1841-1849.

Wilson, J. P., and J. C. Gallant. 2000. *Terrain Analysis: Principles and Applications.* New York, N.Y.: John Wiley and Sons.

Wilson, R. C., R. S. Freeland, J. B. Wilkerson, and W. E. Hart. 2005. Interpolation and data collection error sources for electromagnetic induction-soil electrical conductivity mapping. *Applied Eng. in Agric.* 21(2): 277-283.

Wise, S. M. 1998. The effect of GIS interpolation errors on the use of digital elevation models in geomorphology. In *Landform Modelling and Analysis*, 139-164. S. N. Lane, K. S. Richards, and J. H. Chandler, eds. Chichester, U.K.: John Wiley and Sons.

Zhang, Q., and S. Han. 2002. An information table for yield data analysis and management. *Precision Agric.* 83(3): 299-306.